BULK STIFFNESS AND STRENGTH OF LOW-DENSITY FIBROUS COMPOSITES

Fernando Ramirez*, Paul R. Heyliger, and Jim Hamilton*****
***Universidad de los Andes, Bogota, Colombia.**
****Colorado State University, Fort Collins, CO 80523-1372, USA**
*****Johns-Manville Technical Center, Littleton, CO 80127**

Keywords: *Fibrous composites, linear elasticity, random networks, stiffness, strength.*

Abstract

The effective bulk mechanical properties of low-density fiber composites are determined using network and effective continuum models. Low-density composites are formed of fibers, binder, and air, and possess properties that depend strongly upon the characteristics of the individual constituents. The effective stiffness and strength are modeled using a three-dimensional network with specific focus on the nature of the joints that connect the individual fibers and the influence of fiber orientation. In the stiffness calculation, the bonds between fibers are assumed as ideal, and the primary factors that guide the response of the aggregate are fiber length, diameter, stiffness, and orientation. In strength calculations, the behavior and influence of the binder is far more complex. Two models are used to predict bulk failure mechanisms based on fiber strength and binding node strength. Our theoretical predictions showed excellent agreement with experimental results.

1 Background

There have been numerous attempts to model the effective properties of fibrous composites, including the stiffness and strength of paper and three-dimensional fibrous aggregates. The effect of fiber bond strength has been studied by Dodson [1], Page and Seth [2], and Wang et al. [3-4]. Network models for the analysis of these materials have been used by Arbabi and Sahimi [5], Hamlen [6], Rigdahl et al. [7], and Stahl and Cramer [8]. Bulk strength and stiffness estimates have also been examined by Herrmann et al. [9], Heyden and Gustafsson [10], and Sastry et al. [11]. Several of these studies pointed out useful limitations in network models or highlighted discrepancies between theoretical calculations and physical measurements.

In this work, the focus is directed towards evaluating the primary features that influence the bulk mechanical properties of low density fibrous composites (LDFC). The class of composite under study in this work is composed of fibers, binder, and air, with a typical microstructure shown in Figure 1. The parameters of primary interest for these composites include fiber length, diameter, and orientation, along with the ratio of the fiber to binder material in total weight and also the mat density/weight itself. Each of these parameters can be varied to change the bulk properties of the composite. During the manufacturing of a specific class of LDFC, there is a finite amount of binding agent that is available for distribution within the composite. Part of this binder can coat the fiber length or can collect at the junction location between two or more connecting (or nearly so) fibers. The specific size, number, and shape of these binding nodes can greatly determine the overall strength of the final composite when failure is initiated by the fracture of these locations rather than the strength of the fibers themselves. In this study, two separate models are used to predict bulk strength of the aggregate. The first, which has been used in most studies for composites of this type, uses a criterion of sequential fiber failure. In the second, the sequential failure occurs at the binder nodes. For the type of aggregate studied in this work, it is the latter failure mechanism that is the more realistic and also the more complicated to represent. All composites of this class are three dimensional, and our computational model incorporates this reality. However, some composites of this type have a thickness dimension that is far smaller than the edge

lengths of the other two dimensions, and the composite takes on the appearance of a thin sheet with finite thickness. Other composites of this type are fully three dimensional in that they possess similar dimensions in all three coordinate directions. The focus of this study is on geometries that take on a planar form, but representative results are also explored for a fully three-dimensional composite. The bulk of this study is an exploration of the influence of the individual parameters that control strength and elastic stiffness. We also report results of physical measurements on each of these physical properties and compare these with our theoretical predictions.

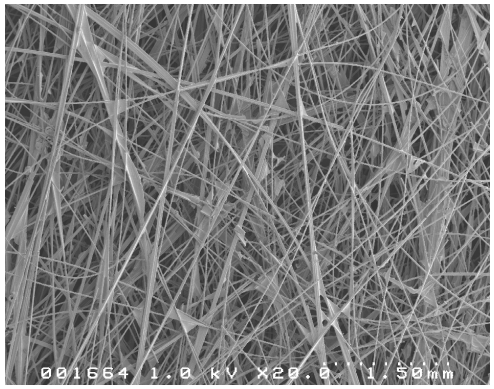

Fig. 1. Microstructure of a LDFC

2 The Network Model

The linear network model is based on the assumptions that the original and final configurations of the composite are essentially the same. Hence the fiber and the network undergo small displacements and small strains, leading to assumptions consistent with linear elasticity theory. The three-dimensional low-density fiber composite is made up of fibers, binders, and air. The fibers are the structural elements, and the binders are the contact points between fibers. The fibrous network is modeled as a collection of one-dimensional line elements (fibers) that possess axial, twisting, and bending stiffness through the material properties E (elastic modulus) and G (shear modulus), the fiber lengths between nodes (L), and the cross-sectional properties of area (A), moments of inertia about the two cross-sectional axes (I_y and I_z) and polar moment of inertia (J). This representation is very common, and the development of the theory can be found in numerous textbooks on finite element analysis or structural analysis. We omit details here, but note that the final result of this process is a system of linear equations of the form

$$[K]\{U\} = \{F\} \tag{1}$$

where $[K]$ is the stiffness matrix, which depends upon all geometric, material, and orientation quantities for all fibers in the aggregate, $\{U\}$ is the vector of nodal displacements, and $\{F\}$ is the global force vector. The joints that connect the fibers at points of crossing are effectively rigid. They possess specific size and contain a limited value of maximum stress that can be applied. There are six components of displacement for three dimensional frame elements at each node. Those components of displacement are three translations and three rotations. Therefore, there are twelve degrees of freedom per element. The additional key parameters that drive the bulk response of the aggregate are the angles the fiber makes with the (x,y,z) axes. These are often random, but can also be controlled to somewhat tailor the behavior of the composite in specific directions. The element equations relating general displacements and forces components are given by

$$[k]\{u\} = \{f\} \tag{2}$$

where $[k]$ is the element stiffness matrix, $\{u\}$ is the nodal displacement component vector, and $\{f\}$ is the force component vector. The element stiffness matrix can be derived by combining the force-displacement relations obtained using the principle of virtual work for axial, shear, bending, and torsion effects. The stiffness matrix for a typical beam element arbitrarily oriented in space, in a local coordinate system, can be found elsewhere, and is a function of the elastic modulus E, the shear modulus G, the cross section area A, the element Length L, the moment of inertia with respect to local y-axis I_y, the moment of inertia with respect to local z-axis I_z, and the polar moment of inertia of the cross section J. The element stiffness matrix must be transformed from the local coordinate system to the global coordinate system using the transformation matrix. The rotation matrix for the forces at the nodes of the beam element are derived based on the angles α, β, and γ that each of the local coordinate axes form with the global X, Y, and Z axes respectively, and it is incorporated into the global statement of equilibrium. Once the element stiffness matrices in global coordinates are obtained, they are combined imposing compatibility of displacements and

equilibrium of forces at each node to obtain a final matrix equation of equilibrium for the complete composite or structure.

3 Predictions of Bulk Properties

The primary quantities of interest in this study are the bulk properties of the composite related to stiffness and strength. These are briefly discussed below.

3.1 Bulk Stiffness

The goal here is to smear the properties of the fibrous composite to simulate that of a continuum, and thus compute the effective bulk properties of the composite. This is accomplished by first defining a control volume *V* around a specific collection of fibers. Those fibers that intersect one of the six faces of the box determine the points that are then defined as boundary nodes, at which locations the resultant forces can be computed. The assumption of affine motion is then invoked. This means that the displacements around the surfaces of the control volume conform to the following relation:

$$u_i = \varepsilon_{ij} x_j \tag{3}$$

Here *u*, ε, and *x* are the components of displacement, strain, and position, respectively. Note that indicial notation is employed, and repeated indices indicate summation. Since stresses cannot be computed at any arbitrary point within the solid since most of the control volume consists of air with the remainder composed of binder and fiber, the forces on the boundary can be computed to yield an effective bulk stiffness assuming that the entire control volume is composed of a linear elastic solid. A statement of virtual work is constructed for the composite under this assumption, yielding

$$\int_V \sigma_{ij} \delta\varepsilon_{ij} dV = \sum_{j=1}^{n} F_{ij} \delta u_i \tag{4}$$

Here σ is stress and *F* are the components of force on the exterior surface of the control volume, and δε and δ*u* are the variations of strains and displacements respectively. If we assume that the stress within a control volume is constant, combining Equations (3) and (4) yields an expression for internal stress as

$$\sigma_{ij} = \frac{\sum_{j=1}^{n} F_{ji} x_i}{V} \tag{5}$$

This formula is extremely useful in providing an estimate of average stress within the composite, yielding a measure for the effective stiffness. The components of an effective elastic stiffness tensor can then be easily obtained by subjecting the composite model to different strain states, performing structural analyses of the network, and evaluating the stress using Equation (5). Finally, the elements of the stiffness matrix C_{ij} are evaluated using the stress strain relationship given by the constitutive equations

$$\sigma_{ij} = C_{ij} \varepsilon_{ij} \tag{6}$$

The elements of the stiffness matrix are determined one column at a time. For example, the first column is obtained by subjecting the network model to a strain state given by $\varepsilon_{11} \neq 0$ with all other $\varepsilon_{ij}=0$.

3.2 Bulk Strength

There are two primary modes of failure in a LDFC. The first is when the axial stress in a fiber exceeds the ultimate strength of the material. The second is where the binding node material fails, resulting in a loss of effective composite action and the subsequent progressive failure of the aggregate. We have constructed models of both mechanisms, and present a brief description below.

3.2.1 Fiber Failure Model

When the binding nodes are sufficiently strong, the means of load transfer through a LDFC is primarily through the axial stretch of the fibers within the aggregate. Although bending and twist are allowed and can physically occur, these effects are small relative to the axial deformation and force within each fiber. As the load increases within a LDFC, the fibers that are the stiffest (i.e. highest modulus and area with the shortest length and orientation most parallel to the action of the load) attract most of the load. As the loading increases, the internal forces increase in effectively linear fashion until a state of first-fiber-failure is reached. At this point, the fiber is computationally allowed to fail by removing it from the subsequent analyses. The loads are then re-distributed within the aggregate as

subsequent load steps are imposed. This class of model is not new, and in fact was used to study another class of LDFC by Stahl and Cramer [8]. It can be an excellent model if the bond strength between fibers is large. However, for the class of composite of most interest in this work, experimental evidence indicates that it is the failure of the nodes the responsible for the overall failure of the composite.

3.2.2 Node Failure Model

A typical failure zone for a LDFC is shown in Figure 2. The traits that are clearly observed in this figure are typical of other failure zones, and show that rather than fiber failure, the primary failure mechanism is the fracture of the binding node locations.

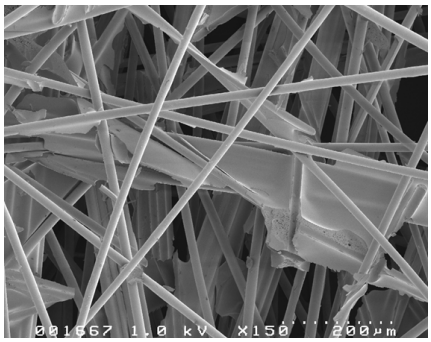

Fig. 2. Typical node failure

Modeling this type of failure mechanism requires knowledge of 1) the strength of the bond between the bond and the fiber, 2) the size of the binder node location, 3) the shape of the binder node, and 4) the distribution of the binder at each location within the aggregate. The first of these parameters has been determined by experiment. The latter three items vary widely between differing nodes and also differing composites. It would be a difficult and tedious process to physically reconstruct the exact size, shape, and distribution of each node within a LDFC for purposes of analysis. In this study, we simplify the procedure by assuming uniform size, shape, and distribution of the nodes. There is no question that this assumption influences the overall behavior, but our main goals are to 1) assess the validity of this model by determining physical estimates of the composite breaking strength, and 2) comparing these results with experimental measurements. The assumptions used in this study yield a uniform node distribution given a certain amount of binder and fibers. The volume of the binder forming each node is the same for all nodes in the network.

The primary model used to represent the bond is based on the assumption that the binding agent coats the fibers with a constant thickness, equal to 10% of the fiber diameter, at locations where two or more fibers cross. This results in a bond area, which is the contacting area the binder makes with the fibers, that can be determined based on the number of intersecting fibers, the assumed binder coating thickness, and the amount of binder available for the formation of the node. Once this area is known, the ultimate strength of the node can be determined using the experimentally measured failure stress between the binder and the fibers.

After the binder locations have been determined, the analysis proceeds in much the same fashion as for the fiber failure model. The load is incremented in a series of steps and the stress at each bond is calculated using the resulting end forces from the analysis. These are compared with the allowable strength of each node. If the induced stress is higher than the allowable value, that node is assumed to fail by removing continuity of the nodal displacements at that location. Although the fibers are left intact, the loss in connectivity yields a redistribution of load within the aggregate composite that will eventually lead to bulk loss in both stiffness and strength.

4. Physical Measurements

Tensile tests were performed by the manufacturer on planar fiber glass mats to determine their Young's modulus and tensile strength. By planar we mean that although the mats have thickness dimension, most of the fibers are primarily contained within the x-y plane and the composites take on the appearance of a thin sheet. A typical physical mat of this class is manufactured with dimensions 254 x 254 x 0.889 mm with a density of 10.48×10^{-5} g/mm^3. The elastic modulus and strength of the glass fibers within this mat are 75.0 GPa and 3.0 GPa, respectively. The fiber lengths are fixed at 25.4 mm, and the diameters are also constant at 0.016 mm. There is no preferred direction of the fibers during manufacturing, and hence the orientation of the aggregate is essentially random. The density of the fibers is 6.23×10^{-4} g/mm^3, with the binder density at 15.0×10^{-4} g/mm^3. The fiber weight fraction within these composites is

0.805. The tensile strength was determined to be 9.19 MPa and the elastic modulus to be 787.73 MPa.

The debonding strength between the fibers and binder has been experimentally measured at 14.38 MPa [12].

5. Applications and Dicussion

The algorithm developed in this study is three-dimensional. However, the nature of the composites studied is largely two-dimensional (effectively, not exactly).

One of the most important steps for the determination of the bulk properties of these composites is the definition of a network geometry that accurately models the actual geometry of the fiber glass mats. The two-dimensional networks are generated based on the actual fiberglass sheet properties related to mat geometry as discussed in the previous section. These parameters include mat thickness, mat density, fiberglass density, fiber weight fraction, fiber orientation, and fiber geometry. A basic fiber network model was constructed based on these primary characteristics with some small changes as discussed below.

The method used to model the composite mat is to first divide the total thickness into a fixed number of layers whose individual thicknesses are equal to twice the fiber diameter. The doubled thickness takes into account the dimension of the binding nodes. A two-dimensional fiber network is then created for each layer of fibers and binder. Each layer satisfies the mass density and fiber weight fraction of the composite as defined by the physical specimen. Each layer of the network is generated by first passing a fiber through a random point inside the model volume. The fiber has an orientation that is generated at random. Two different approaches are employed to manage the sections of the fibers lying outside the control volume. In the first approach they are eliminated from the analysis (i.e. they are cut), and in the second approach periodic boundary conditions are considered. The binder nodes are created by determining the intersection points of the fiber with previous fibers in the current layer. This process is repeated by adding fibers until the mass density and fiber weight fraction of the composite are both satisfied. The final network is then created by laminated adjacent layers to construct a final structural system whose thickness matches the physical composite. The fibers within each layer are only allowed to connect with binder nodes with the fibers located in the corresponding adjacent layers. This modeling mechanism includes the key features of the mat without requiring an excessively large number of nodes, which would drastically slow our analysis procedure.

5.1 Model Size Determination

A fundamental problem with considering a mathematical representation of the full sheet of this composite is computational size. A 10.0 mm square coupon of the fiberglass mat yields a model requiring the solution of about one million degrees of freedom. For the failure model, this would be excessive. To reduce the size of the problem, several networks were created and analyzed. These networks were constructed using 1 to 7 layers using the procedure discussed in the previous paragraph. Results show that if the number of layers within the model is greater than three, there are only small changes in composite behavior and the elastic stiffnesses are nearly the same. It is therefore assumed that three sub-layers are sufficient to model the two-dimensional mats, and this representation is used for all analyses in this section.

A second sequence of analyses was completed to determine the influence of the domain size on the resulting values of stiffness for two-dimensional composites. The fiber length was fixed at 10 mm and the control volume (or area) was adjusted to determine the point at which the side lengths bounding the composite no longer had much influence. Six different side lengths were used: 5, 10, 11, 12.5, 15, and 20 mm. The analyses were completed using periodic boundary conditions, in which fibers that leave the control area at, for example, the right edge then enter the control area at the left edge. The analyses were then repeated without considering periodic boundary conditions. The variable of interest is the C_{11} component of the elastic stiffness tensor. For each computed set of constants, a total of ten analyses were completed with random fiber orientation. The high and low values of the stiffnesses were then eliminated and the final eight values averaged to give the mean response.

As expected, the stiffness decreases slightly as the control area increases. However, the changes in stiffness appear to taper off somewhat when the edge length is approximately 1.1 times the length of the fiber. We attribute the slight increase for the

fiber length of 12.5 to the random nature of the mesh generation. There was very little influence of non-periodic boundary conditions when the control area is this large. We conclude that as long as the domain edge is at least 1.1-1.5 times the length of the fiber, the influence of edge size and boundary type is negligible. This value is used to determine the minimum edge length of our control volume in subsequent analyses.

As a result of the previously described analyses, and to make the problem size more reasonable, the parametric studies to determine the influence of different parameters on the overall stiffness and strength of the fiber composites are performed on network models formed by three basic layers. The total thickness depends on the fiber diameter, with a side length of 10 mm, and a minimum side to fiber length ratio of 1.5. A typical fiber network is shown in Figure 3.

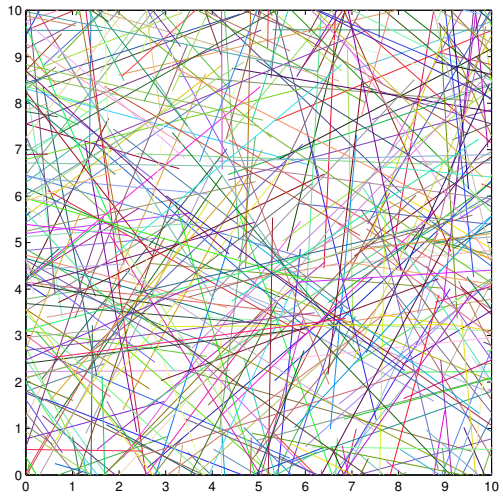

Fig. 3. Typical fiber network constructed based on the

5.2 Bulk Elastic Constants and Strength: Comparison with Physical Measurements

The two-dimensional analyses are initiated with a representative construction of a typical mat. The intent is to use this initial modeling effort to assess the relative level of accuracy for the bulk elastic constants for composite using physically realistic quantities. The values used in this preliminary study are designed to replicate those of the mat used in the experiments discussed in a previous section. The dimensions of the control volume are 27.94 mm x 27.94 mm x 0.0988 mm. The side dimensions match the ratio of edge length to fiber length of 1.1. The remaining fiber parameters are identical to those of the physical sheet described in the previous section. A total of five different random mesh networks were developed using these basic properties, with the elements of the elastic stiffness tensor determined using the method discussed previously. The number of nodes used to discretize the aggregate is nearly the same for each of these simulated networks, and is shown in Table 1 along with the average values for the engineering elastic constants. The two values for Young's modulus and those of the Poisson's ratios are both within about five percent of the values computed in perpendicular directions. This is a very reasonable indicator of the expected material isotropy for this number of fibers and analyses. Both values of elastic modulus are within 8 percent of the measured value of 787.73 MPa, and in fact the averaged value of the two primary directions is within 3 percent of this value.

For the case of axial strength our theoretical model predicts an ultimate strength of 8.7 MPa which is about 5% higher than the experimental measurements.

Given the number of variables in this problem and the difficulty of accurately assessing a true bulk area to compute effective stress, these results are considered to be in very good agreement.

Table 1. Effective bulk engineering elastic properties for 5 different network models and the corresponding average. (E and G in MPa)

E_x	E_y	G	ν_{12}	ν_{21}
763.98	737.35	594.65	0.352	0.340
719.64	810.09	565.73	0.306	0.344
741.10	838.33	538.56	0.285	0.323
713.62	729.29	616.81	0.360	0.368
788.11	789.41	545.38	0.306	0.307
745.29	**780.89**	**572.22**	**0.322**	**0.336**

6. Summary and Conclusions

A three dimensional network model was developed and applied to several representative low density fibrous composites. Overall comparisons with experiment yielded very good agreement between theory and experiment. A virtual work statement was used to determine the elements of the elastic stiffness tensor, and two failure models were developed based on fiber and node failure.

The network model developed in this work gave predicted values for the elastic modulus and Poisson's ratio within eight percent of measured values, and a strength prediction for the nodal failure model within five percent of measured values. These results encourage the application of the proposed network model to the material and geometric optimization problem of LDFC, and to the analysis of three-dimensional fibrous networks.

References

[1] Dodson, C. T. J. (1969). The Failure of Bonds during the Fracture of a Random Fibrous Network, Structure, Solid Mechanics, and Engineering Design}, In M. Te'Eni (ed.), 357-366, Wiley-Interscience, London.

[2] Page, D. H., and Seth, R. (1980). The Elastic Modulus of Paper II. The Importance of Fiber Modulus, Bonding, and Fiber Length. TAPPI Journal, 63:113-116.

[3] Wang, C.W., Berhan, L., and Sastry, A.M. (2000). Structure, Mechanics and Failure of Stochastic Fibrous Networks: Part I - Microscale Considerations. Journal of Engineering Materials and Technology, 122:450-459.

[4] Wang, C.W., and Sastry, A.M. (2000). Structure, Mechanics and Failure of Stochastic Fibrous Networks: Part II – Network Simulations and Application. Journal of Engineering Materials and Technology, 122:460-468.

[5] Arbabi, S. and Sahimi, M. (1988). Elastic Properties of Three Dimensional Percolation Networks with Stretching and Bond-Bending Forces, Physical Review B, 38:7173-7176.

[6] Hamlen, R.C. (1991). Paper Structures, Mechanics, and Permeability: Computer Aided Modeling, University of Minessota, Ph.D. Dissertation.

[7] Rigdahl, M., Westerlind, B., and Hollmark, H. (1984). Analysis of Fiber Networks by the Finite Element Method. Journal of Material Science, 19:3945-3952.

[8] Stahl, D.C., and Cramer, S.M. (1998). A Three Dimesional Network Model for a Low Density Fibrous Compose. Journal of Engineering Materials and Technology, 120:126-130.

[9] Herrmann, H. J., Hanson, A., and Roux, S. (1989) Fracture of Disordered, Elastic Latices in Two Dimensions, Physical Review B, 39:637-648.

[10] Heyden, S., and Gustafsson, P.J. (1998). Simulation of Fracture in a Cellulose Fiber Network. Journal of Pulp and Paper Science, 24(5):160-165.

[11] Sastry, A.M., Cheng, X., and Wang, W. (1998). Mechanics of Stochastic Fibrous Networks. Journal of Thermoplastic Composite Materials, 11:288-295.

[12] Drzal, L. T., and Drown, E. K. (2002). Johns-Manville Fiber/Binder Adhesion Measurements, Test Report, Composite Materials and Structures Center Report, Michigan State University, USA.